Research Square

Preprints are preliminary reports that have not undergone peer review.
They should not be considered conclusive, used to inform clinical practice,
or referenced by the media as validated information.

Volcanology, Petrogeochemistry and Mantle Source Constraints of Monogenetic Volcanoes from the Kumba Plain, Cameroon Volcanic Line

Teitchou Merlin isidore
teitchou.merlin@yahoo.fr

institute for geological and mining research

Tchop joseph Legrand
Institute for geological and mining research

Sahabo aboubacar Abdoulaye
institut de recherches geologiques et minieres

Mbossi Ferdinand
institute for geological and mining research

Mendi-wajiba patrick
institute for geological and mining research

Wokenmendam-Nguet pauline
institute for geological and mining research

Research Article

Keywords: Kumba plain, monogenetic volcanism, volcanic plumbing system, crustal contamination, thermal instabilities

Posted Date: June 26th, 2026

DOI: https://doi.org/10.21203/rs.3.rs-10146118/v1

License: This work is licensed under a Creative Commons Attribution 4.0 International License.
Read Full License

Additional Declarations: The authors declare no competing interests.

Volcanology, Petrogeochemistry and Mantle Source Constraints of Monogenetic Volcanoes from the Kumba Plain, Cameroon Volcanic Line

Merlin Isidore Teitchou[1*], Joseph Legrand Tchop[1] , Aboubakar Abdoulaye Sahabo[2] , Ferdinand Mbossi[1], Patrick Mendi[1], Pauline Wokwenmendam-Nguet[1]

1- Institute for Geological and Mining Research, IRGM / CRGV Ekona, P.O. Box 370 Buea, Cameroon

2- Institut de Recherches Géologiques et Minières, IRGM / CRGM, P.O. Box 4110 Yaoundé, Cameroon

[*]corresponding author (teitchou.merlin@yahoo.fr)

ABSTRACT

The Kumba Plain, located within the continental sector of the Cameroon Volcanic Line (CVL), is a monogenetic volcanic field characterized by basaltic lava flows, scoria cones, and four volcanic lakes (Barombi Mbo, Barombi Koto, Mbwandong, and Disoni). This study integrates volcanological, petrographic, geochemical, and Sr–Nd isotopic data to constrain magma evolution, mantle source characteristics, and the origin of monogenetic volcanism in the region.

Field observations reveal three successive volcanic stages: (i) early fissural eruptions responsible for extensive pahoehoe lava flows, (ii) Strombolian to phreatic/phreatomagmatic activity associated with maar formation and cone construction, and (iii) late localized fissural eruptions producing short cheire lava flows. Two categories of monogenetic volcanoes are distinguished: monogenetic volcanoes sensu stricto (Mbwandong and probably Disoni) and complex monogenetic volcanoes with polygenetic inheritance (Barombi Mbo and Barombi Koto), illustrated by geological maps of late stage evolution of the volcanic plumbing system.

The lavas are predominantly picrobasalts, basanites, alkali basalts, trachybasalts, and doleritic basalts belonging to an incomplete sodic alkaline series. Mineral assemblages consist mainly of olivine, clinopyroxene, plagioclase, and Fe–Ti oxides. Major- and trace-element compositions indicate low differentiation and derivation from low-degree partial melting (≤5%) of an enriched mantle source. Sr–Nd isotopic compositions and incompatible-element patterns suggest a mantle reservoir dominated by HIMU-like characteristics with subordinate EM1 contributions. Crustal contamination was limited, local, and episodic.

The combined volcanological and petrogeochemical evidence indicates that lavas are issues from thermal instabilities microscopically recorded. Thermal instabilities induce rapid magma ascent through lithospheric fractures generated by lithospheric thinning and edge-driven mantle convection beneath the CVL, producing small-volume magma batches and long-lived monogenetic volcanism.

Keywords : Kumba plain, monogenetic volcanism, volcanic plumbing system, crustal contamination, thermal instabilities

I. Introduction

The Cameroon Volcanic Line (CVL; Figure 1A) is one of the most remarkable intraplate volcanic provinces in Africa. It extends for nearly 1,600 km from the islands of the Gulf of Guinea to the continental interior of Central Africa along a NE–SW trend and comprises both oceanic and continental volcanic sectors [1,2]. Volcanic activity along the CVL has persisted from the Cretaceous to Recent times, making it a long-lived magmatic province characterized by considerable temporal and compositional diversity. The continental segment of the CVL, commonly referred to as the "CVL proper", extends south of Mount Oku and includes several major polygenetic volcanic edifices such as Mount Cameroon, Rumpi Hills, Manengouba, Bambouto and Bamenda, as well as numerous monogenetic volcanic fields distributed throughout the lowlands and graben systems. Among these volcanic fields, the Kumba Plain constitutes one of the most extensive and best-preserved examples of continental monogenetic volcanism in Cameroon.

Despite decades of research, the geodynamic origin of the CVL remains debated. Several models have been proposed to explain its formation, including lithospheric thinning associated with mantle upwelling, reactivation of inherited Pan-African lithospheric structures, edge-driven mantle convection, and the development of localized mantle diapirs beneath the lithosphere [3–7]. Unlike classical hotspot tracks, the CVL does not exhibit a clear age progression along its length, suggesting that magma generation is controlled by complex interactions between mantle dynamics and lithospheric architecture.

Petrogeochemical investigations have revealed the presence of three main magmatic affinities within the CVL: transitional series [8–10], tholeiitic series [11], and alkaline series [12–14]. The oldest transitional volcanism has been attributed to the interval between approximately 51 and 40 Ma [10], whereas alkaline magmatism became dominant after 40 Ma and has continued to the present day, as illustrated by the recent eruptions of Mount Cameroon [15,16]. Most volcanic centres of the continental lowlands belong to the alkaline series and are characterized by basaltic to mildly evolved compositions.

The Kumba Plain is particularly important because it contains a wide variety of volcanic landforms, including lava flows, scoria cones, maars and maar-diatreme systems. Previous studies conducted on the Barombi Mbo, Barombi Koto and Mbwandong volcanic districts have established their chronology and provided important constraints on magma genesis and mantle source characteristics. Geochemical and isotopic investigations have shown that: (i) some lava batches experienced crustal contamination [17,18]; (ii) magma sources were affected by carbonatitic metasomatism and generated by low-degree partial melting within the garnet–spinel transition zone [18]; (iii) lavas display isotopic affinities commonly interpreted as HIMU-like signatures [19–21,2], involving dominant contributions from the sublithospheric mantle and subordinate contributions from the subcontinental lithospheric mantle; and (iv) the Kumba volcanic field includes a broad spectrum of volcanic structures ranging from maars and maar-diatremes to lava flows, cones and pyroclastic deposits [17, 22–25]. The idea that CVL represents several independant translithospheric mantle diapirs in an aborted rifting process has also been suggested [7].

Although significant progress has been made regarding the geochemistry and chronology of Kumba volcanism, several aspects of its magmatic evolution remain poorly constrained. In particular, the relationships between mantle source composition, magma evolution, crustal contamination, magma ascent processes and eruptive styles are still incompletely understood. Furthermore, the mechanisms controlling the generation of monogenetic volcanic centres and the transition from mantle melting to surface eruption require additional investigation. Understanding these processes is essential not only for reconstructing the volcanic history of the Kumba Plain but also for improving our understanding of monogenetic volcanism throughout the Cameroon Volcanic Line.

This study integrates volcanological observations, petrographic descriptions, whole-rock geochemistry, mineral chemistry and Sr–Nd isotopic data in order to constrain the origin and evolution of Kumba Plain magmatism. Particular emphasis is placed on the relationships between volcanic architecture, magma evolution and mantle source characteristics. The objectives of this study are therefore to: (i) characterize the eruptive styles and volcanic evolution of the Kumba Plain volcanic system; (ii) establish the petrographic and geochemical characteristics of its basaltic lavas; (iii) constrain mantle source composition and melting conditions using trace-element and isotopic

systematics; and (iv) discuss the implications of these results for the origin of monogenetic volcanism along the Cameroon Volcanic Line and, more broadly, within the intraplate magmatic context of the African Plate.

II. Field Description, Geographical and Geological Setting

The Kumba Plain (4°25'–4°55' N and 9°15'–9°40' E; Figure 1B) is located in the South-West Region of Cameroon between Mount Cameroon and the Rumpi Hills. It constitutes one of the major lowland volcanic provinces of the continental sector of the Cameroon Volcanic Line (CVL) and forms part of a series of graben structures alternating with uplifted horsts along the volcanic line. The plain, commonly referred to as the Meme Valley, covers approximately 1,000 km² and has an average elevation of about 500 m above sea level. Morphologically, it belongs to a vast peneplain that connects the drainage basins of the Mungo and Meme rivers.

The Kumba Plain is characterized by remarkable volcanic diversity. It contains approximately 47 volcanic cones ranging from 20 to 700 m in height [17], numerous lava flows, and four volcanic lakes: Barombi Mbo, Barombi Koto, Mbwandong, and Disoni. The principal structural trend of the plain is approximately N30°E, closely parallel to the general orientation of the Cameroon Volcanic Line. The distribution of volcanic centres and eruptive products suggests a strong structural control exerted by regional fault systems and inherited lithospheric discontinuities.

Two main generations of lava flows can be distinguished in the field. The oldest lava flows are represented by extensive pahoehoe-type basaltic flows that rest directly upon the crystalline basement. These flows are generally dark grey to black, massive in appearance, and locally display well-developed columnar jointing with pentagonal or hexagonal prisms. Their broad areal extent indicates relatively high lava mobility and eruption volumes. Field relationships suggest that these early flows preferentially exploited pre-existing topographic depressions and drainage networks, flowing predominantly from north to south.

The younger lava flows are typically of the cheire type and differ markedly from the older flows by their rough surface morphology, limited spatial extent, and fresher appearance. These flows commonly contain millimetre- to centimetre-sized xenoliths derived from both the continental crust and the upper mantle. They may be massive or highly chaotic and generally form shorter lava fields, typically ranging from approximately 0.3 × 0.6 km to 1.6 × 0.8 km in extent. Compared with the older flows, they are thinner and display weaker weathering development, indicating a younger age.

The volcanic field was emplaced upon a heterogeneous Precambrian basement composed predominantly of granito-gneissic complexes, migmatites, amphibolites, quartzites, and Pan-African granitoids. This crystalline basement exhibits significant lithological and mechanical heterogeneity and likely played an important role in controlling magma ascent pathways and the localization of eruptive centres. In the southern and western sectors of the plain, the basement is locally overlain by sedimentary formations belonging to the Douala Basin, consisting mainly of Cretaceous to Cenozoic sandstones, shales, and marginal marine deposits [26–28].

Volcanic activity in the Kumba Plain is expressed through a variety of monogenetic volcanic landforms, including lava flows, scoria cones, tuff rings, and maars. The spatial distribution of these eruptive centres commonly follows major structural discontinuities, indicating that magma ascent was strongly influenced by inherited crustal fractures and regional stress fields. Such structural control is consistent with models of monogenetic volcanism in which magma supply rate and tectonic stress interact to determine eruptive style and vent distribution [29].

Available geochronological data indicate that volcanic activity in the Kumba Plain began during the Eocene and continued intermittently until the Late Quaternary [17, 23]. This prolonged volcanic history suggests that the region was repeatedly affected by small-volume magma injections generated from a long-lived mantle source. The coexistence of extensive fissural lava flows, Strombolian cones, phreatomagmatic deposits, and maar systems further indicates significant temporal variations in magma supply, magma-water interaction, and eruptive dynamics throughout the evolution of the volcanic field.

The combination of diverse volcanic morphologies, abundant lava flows, well-preserved phreatomagmatic structures, and excellent exposure conditions makes the Kumba Plain one of the most suitable areas within the

Cameroon Volcanic Line for investigating the relationships between mantle processes, magma evolution, and monogenetic volcanism.

III. Sampling Strategy and Petrographic Characteristics

III.1. Sampling Strategy

Representative volcanic samples were collected throughout the Kumba Plain in order to cover the principal volcanic centres, lava-flow units, eruptive facies, and petrographic varieties recognized in the field. Sampling focused primarily on fresh rocks in order to preserve primary mineralogical and geochemical characteristics. Particular attention was paid to lava flows, pyroclastic deposits, scoria cones, and doleritic facies exposed in road cuts, quarries, stream sections, and natural outcrops.

The investigated volcanic centres include Barombi Kang, Barombi Mbo, Kake, Small Ekombe, Mbwandong, Baduma, Bakundu, Ikiliwindi, Bakumba, and Disoni. A total of 75 representative samples were selected for petrographic, geochemical, and isotopic analyses. Weathered surfaces were systematically removed prior to sample preparation to minimize the effects of secondary alteration. Xenolith-bearing samples were also collected to evaluate potential magma–crust interactions and to assess the significance of crustal and mantle components entrained during magma ascent.

Petrographic observations were carried out using transmitted and reflected light microscopy on standard thin sections. Textural relationships, mineral assemblages, disequilibrium features, and secondary alteration products were carefully documented in order to constrain magma evolution, crystallization conditions, and ascent processes.

III.2. Petrographic Characteristics

The volcanic rocks of the Kumba Plain are predominantly basaltic and display a wide range of textures reflecting variations in cooling rates, crystallization histories, and emplacement conditions. The primary mineral assemblage consists mainly of olivine, clinopyroxene, plagioclase, and Fe–Ti oxides. Accessory phases include apatite and, locally, rare leucite. Secondary minerals comprise iddingsite, serpentine, calcite, epidote, and iron hydroxides, which formed during late-stage hydrothermal alteration and weathering.

Petrographic observations indicate that Fe–Ti oxides were among the earliest crystallizing phases, followed by olivine and clinopyroxene, whereas plagioclase generally crystallized during later stages of magma evolution [17, 30]. This crystallization sequence is consistent with the geochemical evolution observed in the investigated basaltic suite. Two principal textural groups can be distinguished (Figure 2a–c):

III.2.1. Microlitic Basalts

Microlitic textures are the most abundant and include porphyritic, weakly porphyritic, and aphyric varieties. Phenocrysts are commonly embedded within a fine-grained microlitic groundmass composed of plagioclase, clinopyroxene, opaque minerals, and locally volcanic glass.

Porphyritic basalts contain abundant olivine and clinopyroxene phenocrysts, whereas weakly porphyritic varieties are characterized by lower phenocryst content. Aphyric basalts contain few or no visible phenocrysts and are dominated by fine-grained groundmass minerals. These textures indicate relatively rapid cooling and emplacement at or near the Earth's surface.

III.2.2. Doleritic Basalts

Doleritic basalts are characterized by intergranular to subophitic textures and the virtual absence of volcanic glass. Their coarser grain size indicates slower cooling rates and crystallization under subvolcanic conditions or within

shallow intrusive bodies. Doleritic facies are less abundant than microlitic basalts but provide valuable information regarding magma storage and crystallization processes prior to eruption.

III.3. Disequilibrium Textures and Magmatic Processes

Several petrographic features indicate that the Kumba magmas evolved under conditions of limited equilibrium and experienced rapid ascent toward the surface (Figure 2: 1–8).

These features include:

- normal and oscillatory zoning in plagioclase and clinopyroxene;
- skeletal and hopper olivine crystals;
- glomeroporphyritic aggregates;
- resorption textures;
- reaction rims;
- quench textures;
- symplectitic intergrowths;
- fractures and microcracks affecting phenocrysts.

Oscillatory zoning and abrupt compositional variations suggest fluctuations in magmatic conditions during crystallization, including changes in temperature, pressure, volatile content, or magma recharge. Skeletal crystal morphologies and quench textures indicate rapid cooling and crystallization, whereas glomerocrysts likely reflect crystal accumulation or syn-eruptive aggregation processes.

Collectively, these petrographic features point to short magma residence times and rapid ascent through the crust, limiting extensive fractional crystallization and preserving primitive mineral assemblages.

III.4. Enclaves and Xenoliths

Several lava flows contain abundant enclaves and xenoliths that record interactions between ascending magma and the surrounding lithosphere (Figure 2: 4–8). Four principal types are recognized:

III.4.1. Crustal Xenoliths

Crustal xenoliths derived from the granito-gneissic basement and, locally, sedimentary formations are common, particularly within the Baduma road section. These xenoliths consist of mono- or polycrystalline aggregates of quartz, feldspar, biotite, amphibole, and accessory minerals. Their presence demonstrates mechanical incorporation of crustal material during magma ascent.

III.4.2. Xenocrysts

Isolated xenocrysts of orthopyroxene, clinopyroxene, olivine, calcic plagioclase, and Fe–Ti oxides occur in several basaltic samples. These crystals may represent disaggregated mantle xenoliths, fragments of lower-crustal lithologies, or crystals inherited from earlier magmatic stages.

III.4.3. Cognate Enclaves

Some volcanic rocks contain enclaves compositionally similar to the host lava. These cognate enclaves probably represent fragments of earlier-crystallized magma batches incorporated into younger ascending magmas.

III.4.4. Mantle Xenoliths

Mantle xenoliths are represented predominantly by peridotitic nodules and fragments entrained within basaltic lavas. They occur either as isolated xenoliths enclosed within lava flows or as peridotite-core volcanic bombs surrounded by a thin basaltic coating. Individual xenoliths range from millimetric to centimetric dimensions and may reach several centimetres in diameter [22].

The preservation of mantle xenoliths indicates rapid magma ascent from mantle depths, limiting thermal equilibration and disaggregation during transport. Their occurrence therefore provides important evidence for direct connections between mantle melting regions and surface eruptions within the Kumba volcanic field.

III.5. Petrographic Classification of the Lavas

The classification adopted for the Kumba Plain lavas is based on:

1. modal proportions of phenocryst phases;
2. textural characteristics;
3. whole-rock geochemical compositions;
4. the nomenclature proposed by Le Maitre et al [31].

Modal mineral abundances were determined using optical point counting (1,000 points per thin section), digital image analysis, and, where appropriate, mass-balance calculations using PETMIX software [32] following the approach of Le Maître [33].

Based on these criteria, the investigated volcanic rocks can be classified into:

- olivine-rich basalts;
- olivine–clinopyroxene-rich basalts;
- ankaramites;
- trachybasalts;
- doleritic basalts.

From an eruptive perspective, two major categories are recognized:

- projected basalts (pyroclastic products);
- flowed basalts (lava flows).

Projected basalts are generally black, reddish-brown, or chocolate-coloured and commonly contain abundant xenoliths and xenocrysts. They typically exhibit porphyritic, weakly porphyritic, or aphyric microlitic textures. Flowed basalts occur as pahoehoe and cheire lava flows and constitute the dominant volcanic products of the Kumba Plain. The abundance of primitive mineral phases, mantle xenoliths, and disequilibrium textures collectively suggests that the Kumba lavas were derived from relatively primitive magmas that experienced rapid ascent and only limited crustal storage prior to eruption.

IV. Geochemistry

IV.1. Analytical Methods

Whole-rock geochemical analyses were performed on carefully selected fresh samples representative of the main volcanic units of the Kumba Plain. Samples were crushed and powdered using agate mills at the University Paul Sabatier (Toulouse III, France) in order to minimize contamination during sample preparation.

Major and minor elements (Tables 1a and 1b) were determined by X-ray fluorescence spectrometry (XRF) using fused glass discs. Analytical precision is generally better than ±1% for major oxides.

Trace-element concentrations (Table 1c) were measured by inductively coupled plasma mass spectrometry (ICP–MS) following HF–HNO_3 digestion in sealed Teflon vessels. International reference materials (BEN, UB-N, and JP-1) were used for calibration and quality control. Analytical uncertainties are generally lower than 3%.

Trace-element compositions of clinopyroxene and plagioclase crystals (Tables 1d and 1e) were obtained using laser ablation ICP–MS (LA–ICP–MS) coupled to a 266 nm frequency-quadrupled Nd-YAG laser system. Analyses were performed on inclusion-free crystal domains using NIST SRM 610 and 612 standards for external calibration.

Major-element data were recalculated on an anhydrous basis. CIPW normative mineralogy (Table 2) was calculated using a fixed FeO/Fe_2O3 ratio of 0.15 in order to evaluate silica saturation and magma affinity. Rock classification follows the recommandations of Le Bas et al. [34] and Le Maitre et al. [31].

Sr and Nd isotopic analyses (Table 3) were carried out at the University of Saint-Etienne (France) using conventional ion-exchange chromatography and thermal ionization mass spectrometry (TIMS). Analytical reproducibility is better than ±0.00002 for both $^{87}Sr/^{86}Sr$ and $^{143}Nd/^{144}Nd$ ratios. Analytical procedures are described in detail by Teitchou et al. [35].

IV.2. Whole-Rock Geochemistry

IV.2.1. Major Elements

The Kumba Plain lavas are characterized by relatively low silica contents (41.92–47.92 wt.% SiO_2), consistent with mafic alkaline magmas. Total alkali concentrations ($Na_2O + K_2O$ = 2.3–7.5 wt.%) indicate a predominantly alkaline affinity. In the TAS diagram (Figure 3), samples plot within the fields of picrobasalts, basanites, alkali basalts, and trachybasalts, defining an incomplete alkaline differentiation trend [36].

MgO contents range from 5.35 to 12.32 wt.%, indicating that many samples retain relatively primitive compositions. The overall compositional range suggests limited magma differentiation. TiO_2 concentrations (2.6–3.8 wt.%) are typical of intraplate alkaline basaltic magmas and comparable to values reported for ocean island basalts (OIB) [37,38].CIPW normative calculations reveal predominantly nepheline-normative compositions, confirming silica-undersaturated alkaline affinities. Only sample I2 contains normative quartz, indicating local silica enrichment and suggesting limited crustal assimilation during magma evolution. Differentiation indices (DI = normative Qtz + Ne + Le + Ab + Or; [39]) range from 17.23 to 43.13, indicating weakly evolved magmas. Normative compositions include nepheline, hypersthene, quartz, and locally perovskite (Table 2). The occurrence of both nepheline- and hypersthene-normative basalts reflects slight variations in magma evolution and contamination processes rather than fundamentally different magma sources. Overall, major-element compositions indicate derivation from relatively primitive alkaline basaltic magmas that experienced only moderate fractional crystallization prior to eruption.

IV.2.2. Trace Elements

Trace-element concentrations are characterized by pronounced enrichment in incompatible elements relative to compatible elements. Primitive mantle-normalized multi-element diagrams (Figure 4) display strong enrichment in large-ion lithophile elements (LILE; Rb, Ba, K) and high-field-strength elements (HFSE; Nb, Ta, Zr, Hf), typical of intraplate alkaline magmatism and OIB-type geochemical signatures [1, 2].

Variations in trace-element ratios such as La/Nb, Zr/Nb, Y/Nb, and Nb/Y are relatively limited and suggest a broadly homogeneous mantle source. These variations are interpreted primarily as reflecting differences in the degree of partial melting rather than major source heterogeneity.

The enrichment of incompatible elements, combined with pronounced LREE enrichment relative to HREE, indicates derivation from low-degree partial melting of an enriched mantle source. Geochemical modelling and trace-element systematics suggest melting degrees generally lower than approximately 5% (see below).

The Nb/Y versus Zr/Y discrimination diagram (Figure 5 and references therein [40-41]) places most samples within a field characterized by enriched mantle signatures, consistent with previous isotopic interpretations proposed for CVL magmatism.

IV.2.3. Mineral Chemistry

Clinopyroxene crystals display variable trace-element concentrations and well-developed rare earth element (REE) patterns (figure 6). Chondrite-normalized REE distributions (Figure 6) are characterized by enrichment in light rare earth elements relative to heavy rare earth elements and closely resemble those observed in the corresponding whole-rock compositions.

Values of $(La/Sm)_N$, $(Sm/Yb)_N$, and $(La/Yb)_N$ indicate crystallization from alkaline magmas derived from an enriched mantle source. The similarity between mineral and whole-rock REE patterns suggests that clinopyroxene crystallized in equilibrium or near-equilibrium with the host magma.

Plagioclase crystals contain relatively low concentrations of compatible transition elements but display variable concentrations of incompatible trace elements $[La/Sm]_N$: 0.77-5.50; $[Sm/Yb]_N$: 1.17-6.23; and $[La/Yb]_N$: 3.27-6.45. These variations are interpreted as reflecting progressive crystallization within a cooling magma system characterized by limited differentiation and relatively rapid ascent.

Together, the mineral chemistry data support petrographic evidence for weakly evolved basaltic magmas and limited crustal storage.

IV.2.4. Sr–Nd Isotopic Characteristics

The Sr–Nd isotopic compositions of the Kumba Plain lavas exhibit a restricted range of variation. Measured $^{86}Sr/^{87}Sr$ ratios range from 0.703128 to 0.703857, whereas $^{143}Nd/^{144}Nd$ ratios vary between 0.51282 and 0.51288 (Table 3).

Most samples cluster within a narrow isotopic field characterized by low Sr isotopic ratios and relatively radiogenic Nd compositions. This restricted variability indicates derivation from a relatively homogeneous enriched mantle reservoir.

Sample I2 displays a slightly higher $^{86}Sr/^{87}Sr$ ratio than the remaining lavas and coincides with the occurrence of normative quartz. This relationship suggests localized crustal contamination affecting a limited number of magma batches.

The isotopic data are consistent with derivation from an enriched mantle source dominated by HIMU-like characteristics, accompanied by subordinate EM1 contributions. The limited isotopic dispersion indicates that these EM1 contributions were minor and did not significantly modify the overall geochemical signature of the magmatic system.

Collectively, the isotopic and trace-element evidence suggests that the Kumba lavas originated from low-degree partial melting of a heterogeneous but predominantly HIMU-like enriched mantle reservoir, followed by only limited crustal interaction during ascent.

V. Discussion

V.1. Diversity of Monogenetic Volcanoes in the Kumba Plain

The Kumba Plain represents one of the most diverse monogenetic volcanic fields of the continental sector of the Cameroon Volcanic Line. The classification proposed for Kumba monogenetic volcanoes is primarily based on the morphological aspects and dominant eruption styles. These phases may occur at many scales from a single explosion

to an eruptive unit comprising products of multiple explosions from the same eruption style. The effusive activity can also be involved in this genetic classification. In this classification system, the recently recognized polymagmatic or polycyclic behaviour of monogenetic volcanoes, e.g. an eruption fed by more than one batch of magma with distinct geochemical signatures [42,43] or eruptive sequences well reported with layers stratigraphically well discriminated [44] can be integrated. The cooling of eruption styles could then be Hawaiian, Strombolian, violent Strombolian, phreatic/phreatomagmatic and effusive activity. Field observations described above mentioned the existence of 47 volcanic cones, 2 types of flows (fissural and explosive) and 4 maars (Barombi Mbo, Barombi Koto, Mbwandong and Disoni) which the origin may be specify in order to understand the magmatic plumbing system.

The Mbwandong maar (**figure 7A**) has an elliptical shape with approximately 550 m long, 400 m width and a maximum depth of 3 m [45]. We observed only altered volcanic blocs and consolidated ashes within it and surroundings, (no lava flow found), point to classify it as monogenetic volcano sensu stricto with violent Strombolian background. In fact, most samples displaying projected basalts features (e.g. NKB3) were collected in the vicinity of this Lake, suggesting a single eruption.

Barombi Mbo and Barombi Koto maars were formed with a least three eruptive episodes well documented and dated [17], [23], [46] and figures therein) with layers stratigraphically separated by the identified paleosoils and the presence of old and recent lava flows intercalated by typical phreatomagmatic deposits. Therefore they can be classified as complex monogenetic volcanoes with polygenetic inheritance. The volcanic system of the Barombi Koto maar is well described by Tamen et al [23] and the late stage evolution of the volcanic plunbing system presented. In addition, we note that the distance separating the two islets (large and small) of the same volcano is about 25 meters. The small islet is said to have formed only at the location of an adventive vent. Thus, Lake Barombi Koto results from several successive stages of evolution, with its edification constituting the last stage. The phreatomagmatic phase that would have initiated the edification of the crater dominates (abundant tuff rings materials) over the Strombolian phase, with the emplacement of pyroclasts and the basaltic flow of cheire and pahoehoe types on the faulting system (**figure 7B**). Around the lake, we observed almost exclusive presence of volcanic products and soils resulting from their alteration. The interpretative geological map of the Barombi Mbo volcanic district (**figure 7C**) deduced from field observations and measurements, eruptive style and volcanic products described by Chako-Tchamabe et al [47], point to the presence of (1) these two types of polymagmatic volcanoes and (2) faulting system transecting the granito-gneissic basement.

Lake Disoni has a roughly rounded shape and covering an area of 132 ha. The water surface reaches 440 m with a maximum depth of 80 m [45] and a width of 1250 m. It is surrounded on all sides by very steep wooded slopes (70^{o}).The case of Disoni Crater Lake (**figure 7D**) is atypical. In fact, the constitution of the lake flanks is identical. Their lower part is covered with old rocks surmounted by quartz pebbles and old basalts. In the SW sector, we have observed a layer of clay accompanied by quartz, gneiss and fragmented micaschists (debris). Despite the volcanic origin of the lake, neither pyroclastic materials nor recent lavas are found in its surroundings. In our opinion, Lake Disoni is a morphological result from a gaseous explosion (dominant or preponderant phase) that emitted very few releases of materials and whose activity must be recent if we take into account the very steep relief's of the environment and the freshness of the basement debris. Therefore the late stage evolution of this lake may come probably from a vulcanian episode related to the tectonic evolution of the eastern region of the Rumpi hills which is affected by major fractures and whose paroxysm is linked to trachytic volcanism [48]. Considering its particular position which places it in the transitional zone between the Rumpi polygenetic volcano and the Kumba graben, makes the exact determination of its tectonic position complex. If we consider that it belongs to the Kumba graben, we can say that it comes probably from a single phreatic eruption characterized by a preponderance of the gaseous phase, classifying it as a monogenetic volcano sensu stricto.

These volcanic features record a succession of eruptive styles that reflect variations in magma supply, magma ascent conditions, and magma–water interaction. Based on field relationships and volcanic morphology, three principal volcanic stages can be recognized. The earliest stage was dominated by fissural effusive volcanism responsible for the emplacement of extensive pahoehoe lava flows resting directly upon the Precambrian basement. This phase was followed by Strombolian, phreatic, and phreatomagmatic activity, which generated numerous scoria cones and the major crater lakes of the plain. The final stage was characterized by localized fissural eruptions producing short cheire lava flows and small eruptive centres. These observations support the recognition of two categories of

monogenetic volcanoes. The first category corresponds to monogenetic volcanoes sensu stricto, represented by volcanic systems formed during a single eruptive episode and supplied by a single magma batch. Mbwandong and probably Disoni belong to this category. The second category comprises complex monogenetic volcanoes with polygenetic inheritance, represented by Barombi Mbo and Barombi Koto, where stratigraphic relationships indicate multiple eruptive episodes separated by periods of quiescence but linked to the same volcanic plumbing system.

Barombi Mbo and Barombi Koto therefore illustrate the capacity of some monogenetic systems to be reactivated repeatedly over long periods while maintaining relatively small eruptive volumes. This behavior has been reported in several monogenetic volcanic fields worldwide and emphasizes the complexity of magma transport processes beneath apparently simple volcanic centres

V.2. Fractional Crystallization and Magmatic Evolution

Petrographic observations and whole-rock geochemical data indicate that magma evolution within the Kumba Plain was dominated by limited low-pressure fractional crystallization. The mineral assemblage composed of Fe–Ti oxides, olivine, clinopyroxene, and plagioclase records a crystallization sequence typical of alkaline basaltic magmas generated in intraplate settings.

The decrease in MgO, Ba, Cu, and Sc contents (figure 8) from ankaramites and primitive basalts toward trachybasalts reflects progressive removal of olivine and clinopyroxene during crystallization. However, the relatively restricted compositional range of the lavas indicates that differentiation remained limited. Most samples retain primitive geochemical characteristics and show no evidence for prolonged storage within large crustal magma chambers.

Several petrographic features support this interpretation. Mg-rich olivine phenocrysts, clinopyroxene-rich assemblages, skeletal crystal morphologies, zoning, and glomerocrystic aggregates indicate rapid crystallization under disequilibrium conditions. Mantle xenoliths preserved within many lava flows further suggest rapid ascent rates, since prolonged storage would have resulted in their thermal equilibration and disaggregation.

Consequently, the Kumba lavas are interpreted as products of relatively primitive magma batches that ascended rapidly through the crust and experienced only limited fractional crystallization before eruption. Similar evolutionary trends have been reported from other monogenetic volcanic fields of the Cameroon Volcanic Line, including the Tombel, Noun, and Nyos plains [10,49,50].

V.3. Evidence for Localized Crustal Contamination

Although the geochemical signature of the Kumba lavas is predominantly mantle-derived, several lines of evidence indicate that localized crustal contamination occurred during magma ascent. Field observations reveal abundant crustal xenoliths derived from the granito-gneissic basement and sedimentary formations. Petrographic studies also document xenocrysts and mineral fragments incorporated into the host basalts. Geochemically, the occurrence of normative quartz and normative hypersthene in a limited number of samples suggests local modification of magma compositions through assimilation processes.

Sample I2 provides the clearest evidence for crustal interaction. This sample contains normative quartz and exhibits the highest measured $^{87}Sr/^{86}Sr$ ratio within the dataset. Such characteristics are consistent with limited assimilation of crustal material during magma ascent. Similar contamination processes have previously been reported for other volcanic centres of the Cameroon Volcanic Line and elsewhere [17, 18, 44].

Nevertheless, the overall isotopic homogeneity of the Kumba lavas demonstrates that crustal contamination remained limited and episodic. Most samples retain low $^{87}Sr/^{86}$ Sr ratios and preserve typical OIB-like trace-element patterns. Consequently, crustal assimilation is interpreted as a secondary process affecting only a small proportion of magma batches and not significantly modifying the primary mantle-derived geochemical signature.

V.4. Mantle Source Characteristics and Partial Melting

The trace-element and isotopic compositions of the Kumba lavas provide important constraints on mantle source composition and melting conditions. Chondrite-normalized trace-element patterns (figure 4) display strong enrichment in incompatible elements and pronounced LREE enrichment relative to HREE. Such features are characteristic of alkaline magmas generated by low-degree partial melting of an enriched mantle source. Trachybasalts and alkali basalts ($Si0_2$ % > 45 %) stand a little from the general trend of picrobasalts and basanites (suggesting different stage or degree of melting ≤ 5% and subsequent crystallization. (figure 9A and reference therein [17]). The batch melting model; plot of the Kumba lavas in the Sm/Yb versus La/Sm diagram after Gurenko et al [51] indicates that partial melting ratio varies from 1.4 to 3.7% (figure 9B and references therein [52].

The relatively high concentrations of incompatible elements, together with elevated Nb, Ta, Zr, and Hf abundances, indicate derivation from a mantle reservoir distinct from depleted MORB mantle [53-54]. Furthermore, the strong fractionation between LREE and HREE suggests melting in the presence of residual garnet, implying melting within the garnet-bearing portion of the upper mantle (figure 9B).

Sr–Nd isotopic compositions define a restricted field characterized by low $^{86}Sr/^{87}Sr$ ratios and relatively radiogenic Nd isotopic values. This isotopic configuration is typical of intraplate alkaline magmatism and reflects small-scale mantle heterogeneity rather than large-scale mixing processes. These signatures are consistent with an enriched mantle source dominated by HIMU-like characteristics. Minor isotopic variability indicates subordinate contributions from an EM1-type enriched component. The available data therefore support derivation from a heterogeneous enriched mantle reservoir in which the HIMU-like component represents the dominant source contribution, whereas EM1 contributions account for the limited isotopic dispersion observed among samples.

The absence of significant depleted mantle signatures suggests that DMM contributions were negligible during magma generation. Variations among lava compositions are therefore interpreted primarily as reflecting differences in the degree of partial melting and subsequent magma evolution rather than major variations in source composition.

Overall, the geochemical and isotopic evidence indicates that Kumba magmatism originated through low-degree partial melting (≤ 5%) of an enriched mantle source characterized predominantly by HIMU-like affinities and minor EM1 contributions.

V.5. Implications for the Origin of Monogenetic Volcanism along the Cameroon Volcanic Line

The Kumba volcanic field provides important insights into the mechanisms responsible for monogenetic volcanism throughout the Cameroon Volcanic Line. Several observations indicate that magma ascent was rapid and occurred through lithospheric fractures that connected mantle melting regions directly to the surface.

The abundance of primitive mineral assemblages, the preservation of mantle xenoliths, the limited degree of magma differentiation, and the generally weak crustal contamination all point to short crustal residence times. These observations suggest that ascending magma batches were relatively small and travelled rapidly through the lithosphere before eruption.

The spatial distribution of eruptive centres further indicates strong structural control on magma ascent. Volcanic centres are commonly aligned along regional fracture systems and fault zones inherited from earlier tectonic events. These structures likely acted as preferential pathways for magma migration and eruption.

The petrological evidence for rapid ascent is consistent with geophysical models invoking edge-driven mantle convection beneath the Cameroon Volcanic Line [3,4,6]. In such models, lateral mantle flow along the northwestern margin of the Congo Craton generates localized thermal anomalies and promotes asthenospheric upwelling. Partial melting within these thermally perturbed regions produces small magma batches that ascend through lithospheric discontinuities to form monogenetic volcanic centres.

Under this framework, the continental lithospheric thickness is gradually thinned from the Congo Craton (45 Km), Kumba plain (≈ 35 km) till south of mount Oku (22 Km) has evidenced by spectral analysis of Cameroon (**figure 1A**) by Nnange [55] and Nnange et al [56]. Lithospheric thinning (figure 1A), basal thermal erosion, and localized asthenospheric upwelling are regarded as consequences of long-lived edge-driven mantle convection rather than evidence for a classical mantle plume. The resulting magma supply is sufficient to sustain intermittent volcanism over tens of millions of years while preserving the scattered distribution and small eruptive volumes characteristic of monogenetic volcanic fields.

The Kumba Plain therefore represents a surface expression of repeated injections of alkaline basaltic magmas generated within a thermally perturbed enriched mantle domain beneath the Cameroon Volcanic Line. This interpretation provides a coherent explanation for the long duration of volcanism, the predominance of monogenetic centres, the synchronous melt sources and the remarkable geochemical similarity observed among volcanic fields distributed throughout the continental sector of the CVL. The synchronous melt sources are still debate but contrast with geophysical models [57].

VI. Conclusions

The Kumba Plain constitutes one of the most representative monogenetic volcanic fields of the continental sector of the Cameroon Volcanic Line. Integrated volcanological, petrographic, geochemical, and isotopic investigations provide new insights into the evolution of its volcanic system and the origin of its basaltic magmatism.

Field observations reveal a volcanic history characterized by three successive stages: (i) an early fissural effusive phase responsible for extensive pahoehoe lava flows, (ii) Strombolian, phreatic, and phreatomagmatic activity leading to the formation of volcanic cones and crater lakes, and (iii) a late fissural phase producing localized cheire lava flows. These volcanic products define two categories of monogenetic volcanoes: monogenetic volcanoes sensu stricto, represented by Mbwandong and probably Disoni, and complex monogenetic volcanoes with polygenetic inheritance, represented by Barombi Mbo and Barombi Koto.

Petrographic and geochemical data indicate that the volcanic rocks are predominantly picrobasalts, basanites, alkali basalts, trachybasalts, and doleritic basalts belonging to an incomplete sodic alkaline series. Their low differentiation indices, primitive mineral assemblages, and widespread disequilibrium textures indicate limited fractional crystallization and relatively short crustal residence times.

Trace-element distributions and Sr–Nd isotopic compositions indicate derivation from low-degree partial melting (≤ 5%) of an enriched mantle source dominated by HIMU-like characteristics with subordinate EM1 contributions. Crustal contamination was limited, local, and episodic, affecting only a small number of magma batches and leaving the primary mantle-derived geochemical signature largely preserved.

The abundance of primitive mineral phases, mantle xenoliths, and weakly evolved magma compositions suggests rapid magma ascent through lithospheric fractures and limited storage within crustal reservoirs. These observations are consistent with geodynamic models involving edge-driven mantle convection, localized asthenospheric upwelling, lithospheric thinning, and basal thermal erosion beneath the Cameroon Volcanic Line.

Collectively, the volcanological and petrogeochemical characteristics of the Kumba Plain support a model in which long-lived monogenetic volcanism results from repeated injections of small-volume alkaline magma batches generated within an enriched mantle domain and transported rapidly to the surface through structurally controlled pathways.

Acknowledgements

This work was funded by the French embassy in Cameroon (SCAC Yaoundé) and supported by the Institute for Geological and Mining Research, IRGM-Cameroon. Prof J.Y Cottin at St Etienne University (France) is thanked for

providing isotopic data. This paper is a tribute to late prof Tchoua Felix and Dr Nana Richard, academic supervisors of this research note.

"Author Declarations":

-Funding : the research was supported by the French Enbassy SCAC in Yaounde-Cameroon in 2006 for laboratory analyses in Toulouse- France, with the approval of the home institution - Institute for Geological and Mining Research

- first author : conception, fieldwork, investigations, writing, original draft and build research team, second and third authors read manuscript. Michel Gregoire supervises data acquisition during our stay in France (UMR 5563), other authors help to improve drawing of figures and constructive comments.

-as declared in the paper, geochemical data were acquired at the university of Toulouse III, UMR 5563 and isotopic data provided by Prof Cottin of the university of saint Etenne, France. Part of thin sections and fieldwork data obtained in Buea – Cameroon under my leadership.
Data availability: all data analyzed during this study are included in this article.

. Ethics, Consent to Participate, and Consent to Publish declarations: not applicable

Reference cited

[1] Fitton JC (1987) The Cameroon Line-West Africa: a comparison between oceanic and continental alkakine volcanism. Alkaline Igneous Rocks (J. G. Fitton; B. G. J. Upton, eds, Geological Society, London, Special Publication, 30), pp. 273-291

[2] Marzoli A, Picirillio EM, Renne PR, Bellieni G, Iacumin M, Nyobe JB, Tongwa AF (2000) The Cameroon Volcanic Line revisited: petrogenesis of continental basaltic magmas from lithospheric and asthenospheric mantle sources. J Petrol 41:87-109

[3] Reusch AM, Nyblade AA, Wiens DA, Shore JP, Ateba B, Tabod CT, Nnange JM (2010) Upper mantle structure beneath Cameroon from body wave tomography and the origin of the Cameroon Volcanic Line. Geochemistry Geophysics Geosystems 11: Q10W07. https://doi.org/10.1029/2010GC003200

[4] Fantah CAC, Kamga APT, Mouzong MP *(*2024) Structure of the lithosphere beneath Cameroon using global gravity model data: implications for the setting of the Cameroon Volcanic Line. Acta Geophys **72**:689–710. https://doi.org/10.1007/s11600-023-01106-4

[5] Moreau C, Regnoult TM, Déruelle B, Robineau B (1987) A new tectonic model for Cameroon line, Central Africa. Tectonophysics 139:317-334.

[6] Iyasu GB (2017) Geochemical Study of the Cameroon Volcanic Line: Implication for the Genesis of Passive Margin Intraplate Magmatism. Graduate School of Natural Science and Technology (Doctor's Course) Okayama University, 234 p

[7] Teitchou MI, Tchop JL, Grégoire M, Mbossi EF, Nguet PW, Abdoulaye SA, Bekoa A (2022b) Upper Mantle Dynamic and Evolution beneath Lake Nyos Volcano (Cameroon Volcanic Line), Documented by Peridotite Xenoliths Enclosed in Alkali Basalts. International Journal of Geosciences 13:438-463. https://doi.org/10.4236/ijg.2022.136024

[8] Fosso J, Ménard J-J, Bardintzeff J-M, Wandji P, Tchoua FM, Bellon H (2005) Les laves du mont Bangou : une première manifestation volcanique éocène, à affinité transitionnelle, de la Ligne du Cameroun. CR Géosciences 337:315-325

[9] Kuepouo, G., Tchouankoue J.P., Nagao.T., Sato.H (2006). Transitional tholeiitic basalts in the Tertiary Bana volcano–plutonic complex, Cameroon Line J. African Earth Sciences, Vol 45 (3) 318-332

[10] Moundi A, Wandji P, Bardintzeff JM, Ménard J-J, Atouba LC, Mouncherou OF, Reusser E, Bellon H, Tchoua FM (2007) Les basaltes éocènes à affinité transitionnelle du plateau Bamoun, témoins d'un réservoir mantellique enrichi sous la Ligne Volcanique du Cameroun. Eocene transitional basalts of the Bamoun Plateau, evidences of an enriched mantle reservoir below the Cameroon Volcanic Line. Comptes Rendus Géoscience, 339:396-406

[11] Aka FT, Hasegawa T, Nche LA, Asobo NEA, Mimba ME, Teitchou I, Ngwa CN, Miyabuchi Y, Kobayashi T, Kankeu B, Yokoyama T, Tanyileke G, Ohba T, Hell JV, Kusakabe M (2018) Upper Triassic mafic dykes of Lake Nyos, Cameroon (West Africa) I: K-Ar age evidence within the context of Cameroon Line magmatism, and the tectonic significance. J African Earth Sci 141: 49-59

[12] Nkouathio DG, Ménard J-J, Wandji P, Bardintzeff J-M (2002) The Tombel graben (West Cameroon): a recent monogenetic volcanic field of the Cameroon Line. Journal of Afr Earth Sci 35:285-300.

[13] Kamgang P, Chazot G, Njonfang E, Ngongang NB, Tchoua FM (2013) Mantle sources and magma evolution beneath the Cameroon Volcanic Line: Geochemistry of mafic rocks from the Bamenda Mountains (NW Cameroon). Gondwana Research, September 2013:727-74 https://doi.org/10.1016/j.gr.2012.11.009

[14] Njonfang, E., Nono, A., Kamgang, P., Ngako, V. and Tchoua, F.M. (2011) Cameroon Line Alkaline Magmatism (Central Africa): A Reappraisal. Geological Society of America Special Paper 478, 173-191

[15] Déruelle B, Ngounouno I, Demaiffe D (2007) The "Cameroon hotline" (CHL): A unique example of alkaline intraplaque structure in both oceanic and continental lithospheres. Comptes Rendus Géosciences 339:589-600

[16] Ntepe- Nfomou, Ngwa C N, Mbassa B J, Teitchou M I, Ateba-Bekoa (2019) Forecasting future volcanic eruptions at Mount Cameroon within the time interval 2000–2200 Bulletin of Volcanology, 81:36 https://doi.org/10.1007/s00445-019-1295-8

[17] Teitchou MI (2008) Volcanologie, pétrologie et géochimie comparees de quelques plaines continentales (Kumba, Tombel, Noun, Nyos) de la ligne du Cameroun. Ph.D thesis, université Yaoundé-1, Cameroun, 260 p

[18] Asaah ANE, Yokoyama T, Aka FT, Iwamori H, Kuritani T, Usui T, Gountie Dedzo M., Tamen J, Hasegawa T, Fozing EM, Wirmvem MJ, Nche AL (2020) Major/trace elements and Sr–Nd–Pb isotope systematics of lavas from lakes Barombi Mbo and Barombi Koto in the Kumba graben, Cameroon volcanic line: Constraints on petrogenesis . Journal of African Earth Sciences Volume 161. https://doi.org/10.1016/j.jafrearsci.2019.103675

[19] Halliday AM, Dickin AR, Fallick AT, Fitton JC (1988) Mantle dynamics: a Nd, Sr, Pb and isotopic study of the Cameroon line volcanic chain. J Petrol 29:181-211

[20] Lee DC, Halliday AN, Fitton JG, Poli G (1994) Isotopic variations with distance and time in the volcanic islands of the Cameroon Line: evidence for a mantle plume origin. Earth Planet Sci Lett 123:119-138

[21] Sato H, Aramaki S, Kusakabe M (1990) geochemical differences gbetween polygenetic and monogenetic volcanoes in the central part of the Cameroon volcanic Line. Geochemical Journal Japan 24**:**357-370.

[22] Teitchou MI, Grégoire M, Dantas C, Tchoua FM (2007) Le manteau supérieur à l'aplomb de la plaine de Kumba (ligne du Cameroun), d'après les enclaves de péridotites à spinelles dans les laves basaltiques. Comptes Rendus Geoscience 339:101–109. https://doi.org/10.1016/j.crte.2006.12.006

[23] Tamen J, Nkoumbou C, Mouafo L, Reusser E, Tchoua FM (2007) Petrology and Geochemistry of Monogenetic Volcanoes of the Barombi Koto Volcanic Field (Kumba Graben, Cameroon Volcanic Line): Implications for Mantle Source Characteristics. Comptes Rendus Geosciences 339:799-809. http://dx.doi.org/10.1016/j.crte.2007.09.007

[24] Chako-Tchamabé B, Kereszturi G, Németh K and Carrasco-Núñez G (2016) How Polygenetic are Monogenetic Volcanoes: Case Studies of Some Complex Maar-Diatreme Volcanoes, in Updates in Volcanology - From Volcano Modelling to Volcano Geology, Nemeth edit, DOI: 10.5772/63486

[25] Chako-Tchamabé B, Graettinger A, Gountié Dedzo M, Tamen J, Nemeth K, Weber B, Fozing EA, Esquivel J-S, Asaah AE, Youmen D, Ohba T (2023) Influence of deep magmatic source region in the growth of complex maar-diatreme volcanoes, wileyonlinelibrary.com/journal/g.j. https://doi.org/10.1002/gj.4887 .

[26] Cornen G, Bandet Y, Giresse P, Maley J (1992) The nature and chronostratigraphy of Quaternary pyroclastic accumulations from Lake Barombi-Mbo (West Cameroon). J Volcanol Geotherm Res 51:357-374. http://dx.doi.org/10.1016/0377-0273 (92)90108-P

[27] Lassere M (1978) Mise au point sur les granitoides dits ultimes du Cameroun: gisement petrographie et geochronologie. Bull BRGM 2:143-159

[28] Njome MS, Suh CE (2005) Tectonic evolution of the Tombel graben basement, southwestern Cameroon Episodes 2005; 28(1):37-41 https://doi.org/10.18814/epiiugs/2005/v28i1/004

[29] Takada, A. (1994) The influence of regional stress and magmatic input on styles of monogenetic and polygenetic volcanism. J Geophys Res, 99, 13563–73. Doi:10.1029/94JB00494.

[30] Teitchou MI, Gregoire M, Sahabo AA, Mbossi EF (submitted) Alkali basalts form the Kumba plain, view on magmatism and formation model of monogentic volcanoes along the Cameroon volcanic line, J Arabian Geosciences.

[31] Le Maitre P, Bateman P, Keller J, Lameyre J, Le Bas MJ, Sabine PA, Schmid R, Sorensen H, Streickeisen A, Woobley AR, Zanettin B (1989) A classification of igneous rocks and glossary of terms. Recommandations of the International Union of Geological Sciences. Subcommission on the systematics of igneous rocks. Ed by Le Maitre R.W. Blackwell Scientific Publications, 193p

[32] Wright TL, Doherty PC (1970) A linear programming and least squares computer method for solving petrologic mixing problems. Geological Society of America Bulletin 81:1995–2008, http://dx.doi.org/10.1130/0016-7606(1970)81[1995:ALPALS]2.0.CO;2

[33] Le Maitre RW (1979) A new generalised petrological mixing model. Contrib Mineral petrol 71:133-137

[34] Le Bas MJ, Le Maitre RW, Streckeisen A, Zanettin B (1986) A chemical classification of volcanic rocks based on the total alkali-silica diagram. J Petrol 27:745-750

[35] Teitchou MI, Tchop JL, Grégoire M, Wokwomendam-Nguet P, Mbossi EF, Dili-Rake J, Hell JV (2022a) Xenoliths Evidence of Alkaline Magmatic Infiltrations Beneath Lake Nyos (Cameroon Volcanic Line, West Africa). Open Journal of Geology 12:433-459. https://doi.org/10.4236/ojg.2022.12602

[36] Miyashiro A (1978) Nature of alkalic volcanic rock series. Contr Mineral and Petrol 66:91–104. https://doi.org/10.1007/BF00376089

[37] Sun S, McDonough WF (1989) Chemical and Isotopic Systematics of Oceanic Basalts: Implications for Mantle Composition and Processes. Geological Society, London, Special Publications 42:313-345. https://doi.org/10.1144/GSL.SP.1989.042.01.19

[38]Vermeesch P (2006) Tectonic discrimination of basalts with classification trees. Geochimica et Cosmochimica Acta. 54:321-344

[39] Thornton CP, Tuttle OF (1960) Chemistry of igneous rocks. Differentiation index. Amer J Sci 258:664-684.

[40] Weaver B. L. (1991)The origin of ocean island basalt end-member compositions: trace element and isotopic constraints, Earth Planet. Sci. Lett., Vol 104 , pp. 381-397 https://doi.org/10.1016/0012-821X(91)90217-6 **DOI**

[41] Condie, K. C (2005) High field strength element ratios in Archean basalts: a window to evolving sources of mantle plume, Lithos, Vol 79, pp. 491-*504* https://doi.org/10.1016/j.lithos.2004.09.014

[42] Brenna, M., Cronin, S.J., Smith, I.E.M., Sohn, Y.K., Németh, K. (2010) Mechanisms driving polymagmatic activity at a monogenetic volcano, Udo, Jeju Island, South Korea. Contr Mineral Petrol, 160, 931–50. Doi:10.1007/s00410-010-0515-1.

[43] Nemeth, K. (2010) Monogenetic volcanic fields; origin, sedimentary record, and relationship with polygenetic volcanism. Spec Paper Geol Soc Am, 470, 43–66.
Doi:10.1130/2010.2470(04).

[44] Chako –Tchamabé B, Kereszturi G, Németh K, Carrasco-Núñez G (2016) How Polygenetic are Monogenetic Volcanoes: Case Studies of Some Complex Maar-Diatreme Volcanoes
Updates in Volcanology - From Volcano Modelling to Volcano Geology, Nemeth edit, chap 13
http://dx.doi.org/10.5772/63486

[45] Hassert I (1907) les volcans du Cameroun occidental, Bull volcanol, 13, 161-170.

[46] Chako-Tchamabé B, Ohba T, Kereszturi G, Németh K, Aka FT, Youmen D, Miyabuchi Y, Ooki S, Tanyileke G, Hell JV (2015) Towards the reconstruction of the shallow plumbing system of the Barombi Mbo maar (Cameroon) implications for diatreme growth processes of a polygenetic maar volcano. Journal of Volcanology and Geothermal Research 301:293–313. https://doi.org/10.1016/j.jvolgeores.2015.06.004

[47] Chako Tchamabé B, Ohba TI, Ooki S, Youmen D, Owona S, Tanyileke G, Hell J (2014) Temporal Evolution of the Barombi Mbo Maar, a Polygenetic Maar-Diatreme Volcano of the Cameroon Volcanic Line. International Journal of Geosciences 5:1315-1323. https://doi.org/10.4236/ijg.2014.511108

[48] Nkoumbou C (1990) Etude géologique des monts Rumpi, um ensemble plutonique et volcanique de la ligne du Cameroun, donnes petrologiques sur les Nephelinites du Mont Etinde. PhD thesis univ Nancy I, 352p

[49] Nkouathio DG, Kagou Dongmo A, Bardintzeff JM, Wandji P, Bellon H, Pouclet A (2008) Evolution of Volcanism in Graben and Horst Structures along the Cenozoic Cameroon Line (Africa): Implications for Tectonic Evolution and Mantle Source Composition. Mineralogy and Petrology 94:287-303. http://dx.doi.org/10.1007/s00710-008-0018-1

[50] Nana R (2001) Pétrologie des Péridotites en Enclaves dans les Basaltes Alcalins Récents de Nyos: Apport à la Connaissance du Manteau Supérieur de la Ligne du Cameroun. PhD thesis, Yaoundé, Cameroon, University of Yaoundé I, 250 p

[51] GURENKO A; HOERNLE K; HAUFF F; SCHMINCKE H; HAN D; MIURA Y; I. KANEOKA I (2006) Major, trace element and Nd–Sr–Pb–O–He–Ar isotope signatures of shield stage lavas from the central and western Canary Islands: insights into mantle and crustal processes, *Chem. Geol.*, Volume 233 (2006), pp. 75-112 https://doi.org/10.1016/j.chemgeo.2006.02.016

[52] Workman R K and Hart S R (2005) Major and trace element composition of the depleted MORB Mantle (DMM), *Earth Planet. Sci. Lett.*, Volume 231, pp. 53-72

[53] Ballentine CJ, Lee D-C, Halliday AN (1997) Hafnium isotopic studies of the Cameroon line and new HIMU paradoxes. Chemical Geology 139:111-122

[54] Puziewicz J, Sonja A, Ntaflos T, Gerdes A, mazurek H, Kukula A, Tedontefack St, Ziobro-Mikrut M (2023) The origin of the DMM-like lithospheric mantle beneath continent: mantle xenoliths from the Oku volcanic group in the Cameroon Volcanic Line. J Petrology 64 https://doi.org/10.1093/petrology/egad049

[55] Nnange JM (1991) The crustal structure of the Cameroon volcanic line and the Foumban shear zone based on gravity and aeromagnetic data. Ph.D dissertation, University of Leeds, Leeds, UK, 242p

[56] Nnange J.M (2001) Lithospheric structure beneath Cameroon volcanic fields. Tectonophysics 338:1–16.

[57] Ngu CB, Njinju E.A (2026) Lithospheric architecture of the Cameroon Volcanic Line with implications for the asynchronous melt source. Geophysical J Intl 44: 2. https://doi.org/10.1093/gji/ggaf506

Table captions

Table 1.

a- Chemical compositions (major elements) of the lavas from the Kumba plain

sample	T14	E4	E1	B4	K3	T9	MY	M5	M6	
SIO2 (%)	41.93	42.67	43.45	44.45	43.82	43.25	46.38	46.19	46	
TIO2 (%)	3.77	3.21	3.24	3.33	3.34	3.54	2.82	2.95	2	
AL2O3 (%)	10.25	12.25	12.35	13.62	12.76	12.88	13.22	13.14	13	
FE2O3 (%)	13.39	14.11	14.56	14.39	14.41	13.94	13.12	13.26	13	
MnO (%)	0.18	0.18	0.19	0.21	0.21	0.19	0.19	0.18	0	
MgO (%)	10.11	11.06	11.24	7.42	11.1	10.39	10.67	9.8	10	
CaO (%)	14.86	11.15	11.12	12.99	11.07	10.55	10.06	10.36	9	
Na2O (%)	1.35	1.83	2.08	2.21	2.6	2.85	2.54	2.57		
K2O (%)	0.99	1.05	0.95	1.18	1.09	0.92	1.23	1.07	0	
P2O5 (%)	0.76	0.66	0.65	0.54	0.71	0.69	0.69	0.65	0	
Total	97.59	98.16	99.82	100.35	101.1	99.2	100.9	100.17	100	
Mg#	57.37	58.28	57.91	47.9	57.87	57.05	59.18	56.84	58	
DI	17.23	21.64	23.24	25.71	27.41	28.87	28.74	28.16	26	

b- Chemical compositions (minor elements) of the lavas from the Kumba plain (XRF data)

sample	T14	E4	E1	B4	K3	T9	MY	M5	M6	
V (PPM)	325	264	273	356	279	272	235	238	2	
Cr (PPM)	427	323	355	182	354	368	430	438	5	
Ce (PPM)	52	61	65	54	58	57	56	55		
Ni (PPM)	131	178	209	67	219	72	241	202	2	
Cu (PPM)	104	178	116	128	82	172	91	122		
Zn (PPM)	124	112	113	118	116	114	116	124	1	
Ga (PPM)	24	25	27	28	27	23	25	27		
Rb (PPM)	44	30	19	36	28	25	36	23		
Sr (PPM)	1026	808	680	948	730	799	915	752	7	
Y (PPM)	32	25	26	31	28	29	32	33		
Zr (PPM)	425	185	182	299	202	202	280	278	2	
Nb (PPM)	89	43	43	82	49	51	61	55		

Mo (PPM)	0.8	0.1	0.2	1.2	0.7	1.5	1.2	0.3	
Sn (PPM)	5.3	309	18.4	6.4	1.1	730	189	28.3	7
Ba (PPM)	378	269	373	389	303	344	457	323	4
Ce (PPM)	121	43	42	110	67	53	81	82	
La (PPM)	42	0	0	41	5.8	0	34	19	
Hf (PPM)	12	0	3.8	7.6	0	0.9	4.8	4.6	
W (PPM)	30	51	31	35	24	54	28	36	
Pb (PPM)	4.6	9.5	1.7	6.4	0.2	1.9	3	0	
Th (PPM)	17	14	8	15	13	12	13	0	
U (PPM)	11	0	0	0	0	0	0	0	

c- Chemical compositions (trace elements) of the lavas from the Kumba plain (ICP-MS data)

sample	**T14**	**E4**	**E1**	**B4**	**K3**	**T9**	**M5**	**M6**	
Sc (PPM)	40	27	29	33	26	24	23	30	
Ti (PPM)	21752	20575	18931	19593	18996	19790	17018	15138	
v (PPM)	325	264	273	356	279	272	238	222	
Cr (PPM)	427	323	355	182	354	368	438	507	
Co (PPM)	52	61	65	54	58	57	55	57	
Ni (PPM)	131	178	209	67	219	72	202	266	
Cu (PPM)	104	178	116	128	82	172	122	56	
Zn (PPM)	124	112	113	118	116	114	124	116	
Ga (PPM)	22	22	21	23	20	18	21	20	
Rb (PPM)	34	22.3	17.1	27.2	19.3	17.2	22.1	19.2	
Sr (PPM)	1038	867	653	961	693	730	726	690	
Zr (PPM)	413	191	175	291	190	183	264	235	
Nb (PPM)	91	48	43	84	47	47	54	48	
Cs (PPM)	0.3	0.2	0.14	0.21	0.21	0.26	0.21	0.1	
Ba (PPM)	415	330	489	410	342	366	364	447	
La (PPM)	72	31	28	64	33	34	42	40	
Ce (PPM)	149	65	59	124	69	68	85	81	
Pr (PPM)	18	8.2	7.3	14.3	8.7	8.4	10.4	9.8	
Nd (PPM)	70	33	29	52	35	33	40	38	
Sm (PPM)	15.4	8.1	7.2	11.4	8.3	8	9.4	9	
Eu (PPM)	4.2	2.4	2	3	2.2	2.4	2.7	2.6	
Gd (PPM)	9.9	6.1	5.5	7.3	6	6.1	7.2	6.9	
Dy (PPM)	7.6	5.5	4.9	6.2	5.5	5.3	6.1	6	
Ho (PPM)	1.1	0.9	0.8	1	0.9	0.9	1	1	
Er (PPM)	2.5	2	1.7	2.3	2	2	2.5	2.4	
Yb (PPM)	1.9	1.6	1.4	1.8	1.7	1.6	2	1.8	
Lu (PPM)	0.3	0.2	0.2	0.2	0.2	0.2	0.2	0.2	
Hf (PPM)	9.7	4.6	4.3	6.6	4.7	4.4	6.2	5.5	
Ta (PPM)	5.5	2.9	2.6	5	2.9	2.9	3.3	3	

Y (PPM)	31.7	25	25.8	31.3	27.9	28.8	32.5	31.5
Th (PPM)	7	2.9	2.5	6.5	3	3.2	4.2	3.8
U (PPM)	2	0.8	0.7	1.5	0.9	0.9	1.4	1

d- LA-ICPMS chemical analyses of plagioclases of the lavas from the Kumba plain

sample	**MY**	M6	**NKB3**
Sc (PPM)	3.04		
Ti (PPM)	781	602	292
v (PPM)	5.44		
Cr (PPM)	6.76		
Fe (PPM)	3696	2158	2080
Ni (PPM)	1.56		
Rb (PPM)	6.31	4.38	4.66
Sr (PPM)	1304	859	1514
Zr (PPM)	19.69	13.91	5.36
Nb (PPM)	1.52	0.56	0.19
Ba (PPM)	251	123	81
La (PPM)	4.3	2.33	4.3
Ce (PPM)	6.98	3.52	5.64
Pr (PPM)	0.652	0.358	0.51
Nd (PPM)	1.9	1.06	1.25
Sm (PPM)	0.349	0.169	0.201
Eu (PPM)	0.353	0.487	0.434
Gd (PPM)	0.249	0.223	0.239
Tb (PPM)	0.046	0.021	0.021
Dy (PPM)	0.234	0.187	0.187
Ho (PPM)	0.052	0.04	0.036
Er (PPM)	0.145	0.012	0.103
Yb (PPM)	0.151	0.105	0.1
Lu (PPM)	0.022	0.016	0.015
Hf (PPM)	0.573	0.337	0.209
Th (PPM)	0.33	0.2	0.08
U (PPM)	0.31	0.17	0.07

e- LA-ICPMS chemical analyses of clinopyroxenes of the lavas from the Kumba plain

sample	**K3**	**O2**	**NKB3**	**MC4**	**T14**
Sc (PPM)	82	82	99	93	70
Ti (PPM)	11863	13198	13876	19708	15348
v (PPM)	291	316	245	374	215
Ni (PPM)	117	83	108	88	68
Rb (PPM)	0.55	0.96		0.81	1.52
Sr (PPM)	97	113	96	176	204

Y (PPM)	10	12.7	11	16.3	29.6
Zr (PPM)	88	96	114	251	369
Nb (PPM)	0.89	1.69	0.61	2.77	2.77
Ba (PPM)	2.47	8.57	0.59	5.7	16
La (PPM)	4.2	4.07	5.28	12.4	19.7
Ce (PPM)	14	14.4	17.1	37.9	58.6
Pr (PPM)	2.74	2.72	3.16	6.85	10.3
Nd (PPM)	16.2	17	18.5	36.8	49
Sm (PPM)	5.24	5.5	5.71	11.1	13.2
Eu (PPM)	1.77	1.82	1.73	3.16	3.95
Gd (PPM)	5.04	4.98	4.36	8.08	9.82
Dy (PPM)	4.57	4.76	3.92	6.71	7.99
Ho (PPM)	0.74	0.8	0.67	1.03	1.28
Er (PPM)	1.55	1.81	1.49	2.2	2.79
Yb (PPM)	1.06	1.35	1.17	1.76	2.07
Lu (PPM)	0.14	0.17	0.17	0.22	0.26
Hf (PPM)	3.73	4.06	5.11	9.75	14.1
Ta (PPM)	0.11	0.17	0.15	0.44	0.65
Th (PPM)	0.06	0.2	0.1	0.18	1.14
U (PPM)	0.02	0.05	0.02		0.27

Table 2. CIPW normative compositions of lavas from the Kumba Plain

Sample	**Q**	**Or**	**Ab**	**An**	**Ne**	**Di**	**Hy**	**il**	**Ol**	**Hem**	**Ti**	**Ap**	**Per**	**An Pl**	**Total Pl**	**D I**
T14	0	5.83	11.4	19.02	0	34.27	0	4.03	6.51	11.48	1.01	1.75	2.11	63	30.42	17.23
E4	0	6.18	15.46	22.14	0	20	4.11	4.34	9.92	12.48	2.27	1.52	0	59	37.6	21.64
E1	0	5.63	17.61	21.54	0	20.29	2.9	4.35	10.9	12.48	2.33	1.5	0	55	39.15	23.24
B4	0	6.99	18.72	23.75	0	26.12	0	4.35	4.47	12.34	1.29	1.24	0.88	56	42.47	25.71
K3	0	6.43	19.79	19.94	1.2	20.83	0	4.35	1.26	12.35	0	1.64	1.77	50	39.73	27.41
T9	0	5.44	22.61	19.63	0.8	18.32	0	4.18	12.2	11.94	0	1.6	2.28	46	42.24	29.24
MY	0	7.24	21.5	21.04	0	17	7.54	3.97	7.81	11.24	1.79	1.59	0	49	42.54	28.74
M5	0	6.39	21.76	21.18	0	17.94	8.68	5.19	3.99	11.37	2.08	1.5	0	49	42.94	28.15
M6	0	5.73	20.29	22.21	0	16.51	13.8	3.95	3.26	11.18	1.59	1.37	0	52	42.5	26.02
I_2	4.5	4.37	20.31	23.91	0	15.58	12.3	4.21	0	12.04	1.06	1.02	0	54	44.22	29.18
TB	0	7.74	22.75	20.41	0	17.58	2.94	3.96	9.4	11.3	2.22	1.55	0	47	43.16	28.87
K1	0	8.77	28.3	22.55	0	8.54	11.2	4.14	0.91	11.86	3.11	1.58	0	44	50.85	37.07
NKB3	0	10.9	27.77	20.4	4, 5	14.99	0	3.7	4.48	10.26	0	1.88	2,11	42	48.17	43.13

Table 3. Isotopic compositions (Sr, Nd) of lavas from the Kumba plain

Sample	$^{87}Sr / ^{86}Sr$	Error	$^{143}Nd / ^{144}Nd$	Error
K1	0 .703128	0.000007	0.51288	0.000006
M6	0 .703393	0.000009	0.51284	0.000006
T9	0 .703304	0.000009	0.51285	0.000007
I_2	0 .703857	0.000009	0.51286	0.000007
T14	0 .703367	0.000001	0.51282	0.000006

Table 4. Comparative ratios of some trace elements in the lavas of the Kumba plain with those of other alkaline series. Data are from Nkouathio et al. ([12], Tombel), Moundi et al ([10], Noun), Nana ([53], Nyos), Sun and McDonough ([43], OIB) and this study.

	Kumba	Tombel	Noun	Nyos	OIB
Zr/Nb	3.43-6.10	4 -5.1	3.4	3.7	5.8
La/Nb	0.66-0.81	0.68-0.77	0.75	0.78	0.77
Ba/Nb	4.6-11.3	6.2-8.9	10.7	9.76	7.3
Rb/Nb	0.32-0.64	0.36-0.56	0.6	0.42	0.65
Ba/La	5.8-17.3	8.5-12	15.5	8.32	9.46
Zr/Ta	57.6-94.4	54.6-70	-	-	104
La/Ta	13.1-10.5	9.5-10.7	-	-	13.7
Ba/Ta	57-194	80.8-122	-	-	129.6
Th/Ta	0,98-1,36	1-1.2	-	1.1	1.48
La/Th	9.2-11,2	8-10.3	7.7	8.4	9.25
Th/U	3.09-4.39	2.1-4.6	-	2.6	3.92
Ba/Th	58.7-93.9	68-114	119	88	87.5

Figure captions and microphotographs

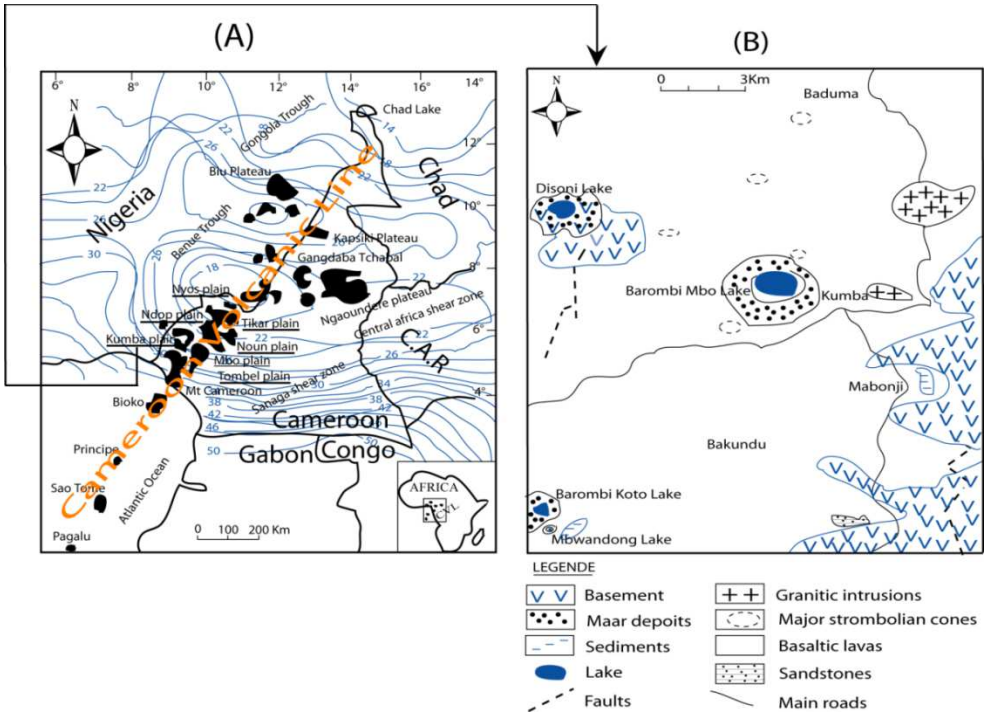
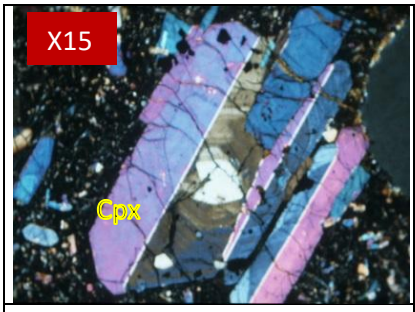
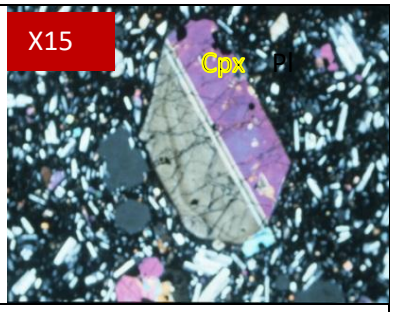


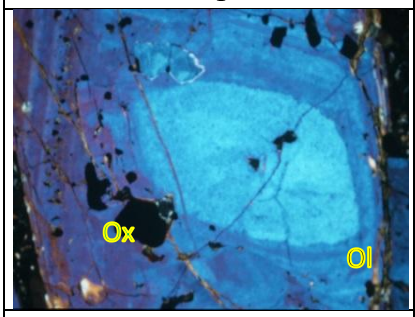
Figure 1. (A). Cameroon Volcanic Line indicating main volcanic plains and crustal thickness (adapted from Nnange [55]) and (B) geological map of the Kumba plain



1



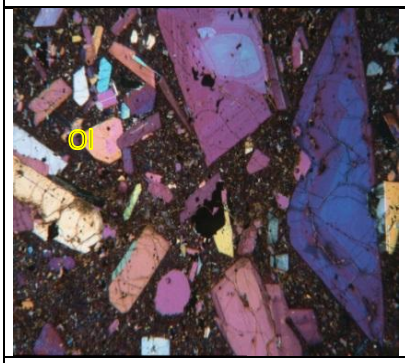
2



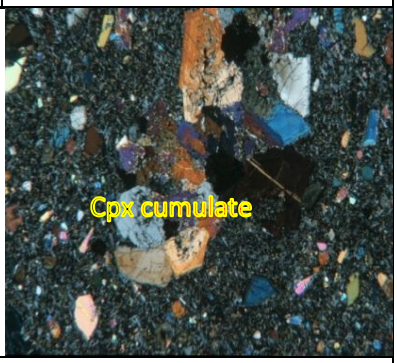
3



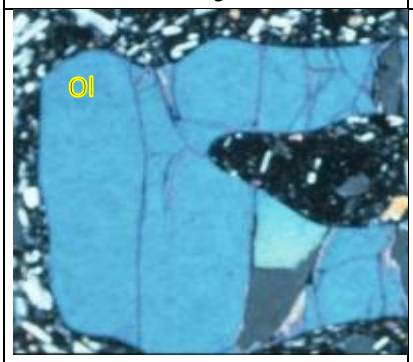
4



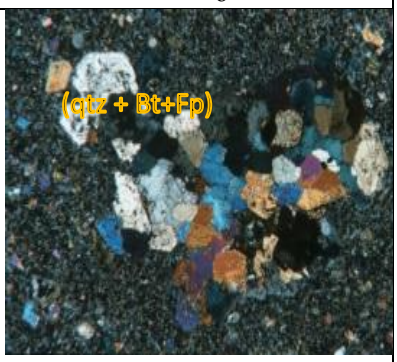
5



6



7



8

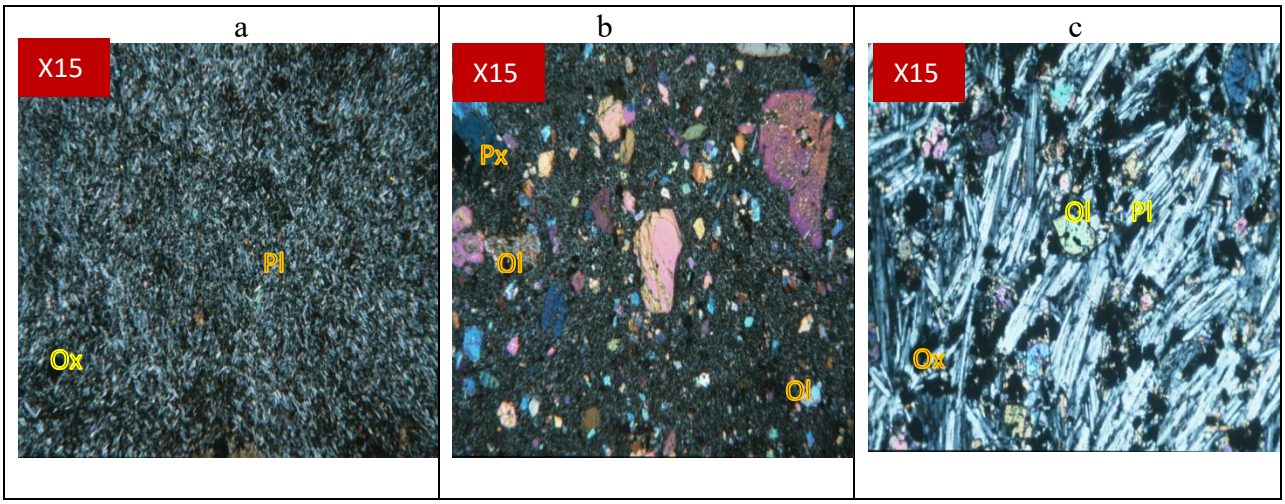


Figure 2. Main deformation figures and enclaves (1-8) and types of outcrops (a, b and c) of the lavas form the Kumba plain (same scale)
1 and 2: Cracked and macled pyroxene phenocrysts with concentric zonation
3: Zoned olivine xenocryst in olivine rich basalt
4: Zoned plagioclase with polysynthetic mackle (sample M3)
5: Glomeroporphyritic aggregate of pyroxenes in a picritic basalt (sample T14)
6: Clinopyroxene cumulate in an olivine and pyroxene rich basalt (sample K2)
7: xenoclast of olivine in imbalance with the magma
8: xenoliths from the granito-gneissic bedrock consisting of quartz (qtz), biotite (Bt) and feldspar (Fp)
a: Microlitic texture in flow basalt (sample M5) ; b: basaltic projection (sample NKB3) and c: doleritic texture (sample MY)

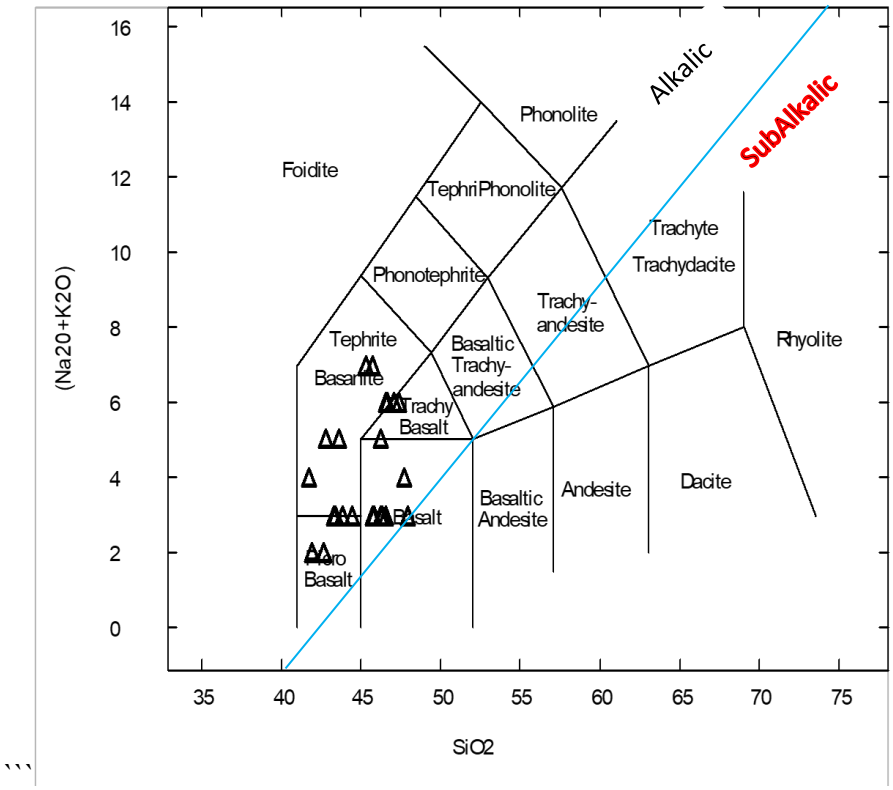


Figure 3. Total Alkali Silica or TAS classification after Le Bas et al [34] of lavas from the Kumba plain. The line separating the alkaline and sub-alkaline fields is after Miyashiro [35]

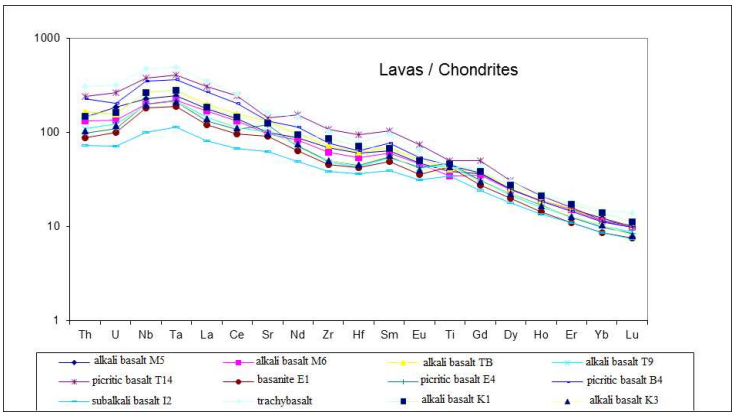


Figure 4. Multi-element abundance patterns normalized to Chondrites of lavas from the Kumba plain. Normalization values after Sun and McDonough [37]

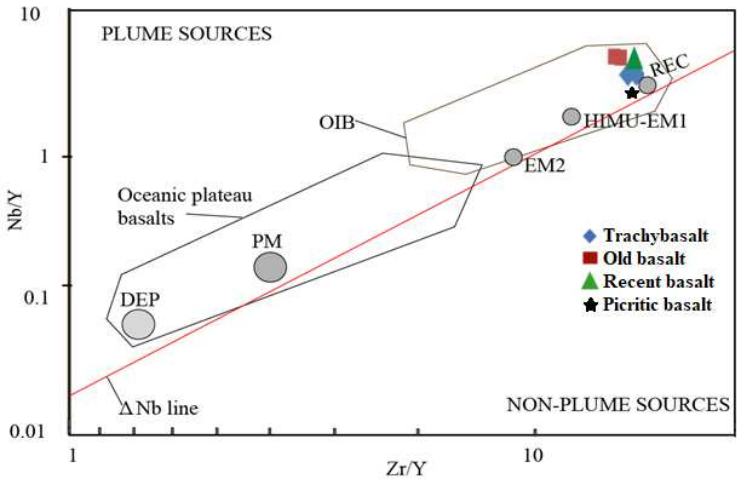


Figure 5. Discrimination of Kumba lavas in relation to various mantle components and basalt fields, as defined by Weaver [40] and Condie [41]. ΔNb line is after Fitton et al [1]. DEP = Deeply Depleted Mantle; REC = Recycled Component; PM = Primitive Mantle, DM =: Depleted Mantle, HIMU = high-μ, EM = Enriched Mantle

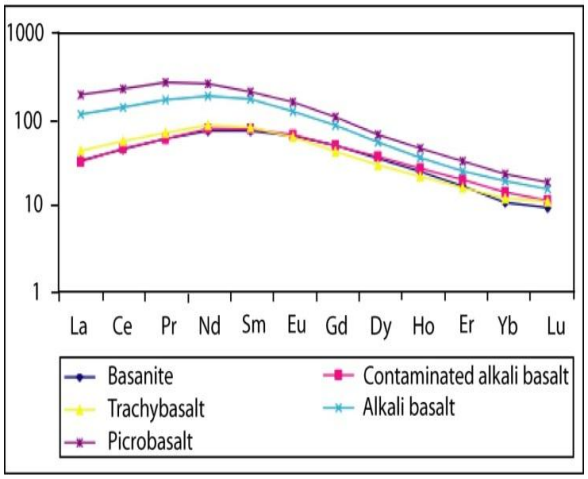


Figure 6. Cpx REE patterns of basaltic lavas from the Kumba plain. Normalization value after Sun and McDonough [37]

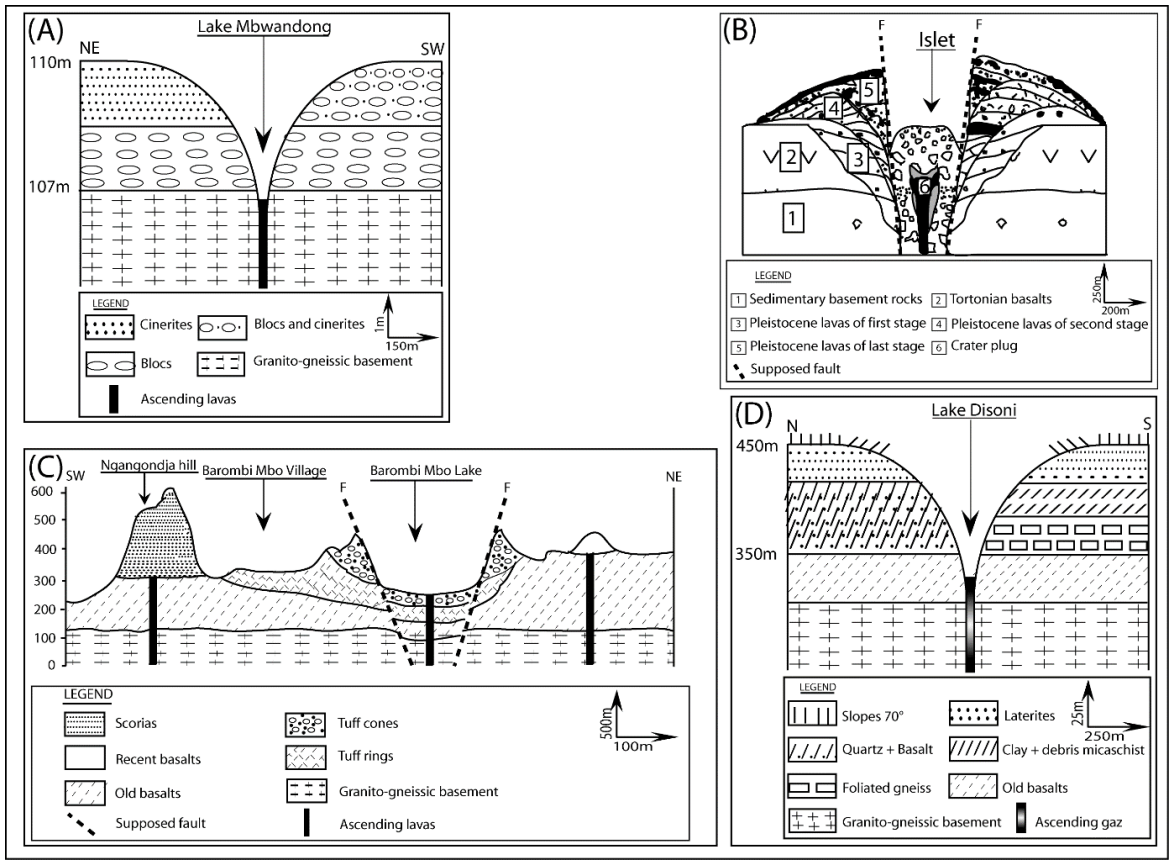


Figure 7. Interpretative geological maps of monogenetic volcanoes with a maar signature from the Kumba plain (late stage evolution of volcanic plumbing system). A: lake Mbwandong volcanic field, B: lake Barombi Koto volcanic field, C: lake Barombi Mbo volcanic field, D: lake Disoni volcanic field

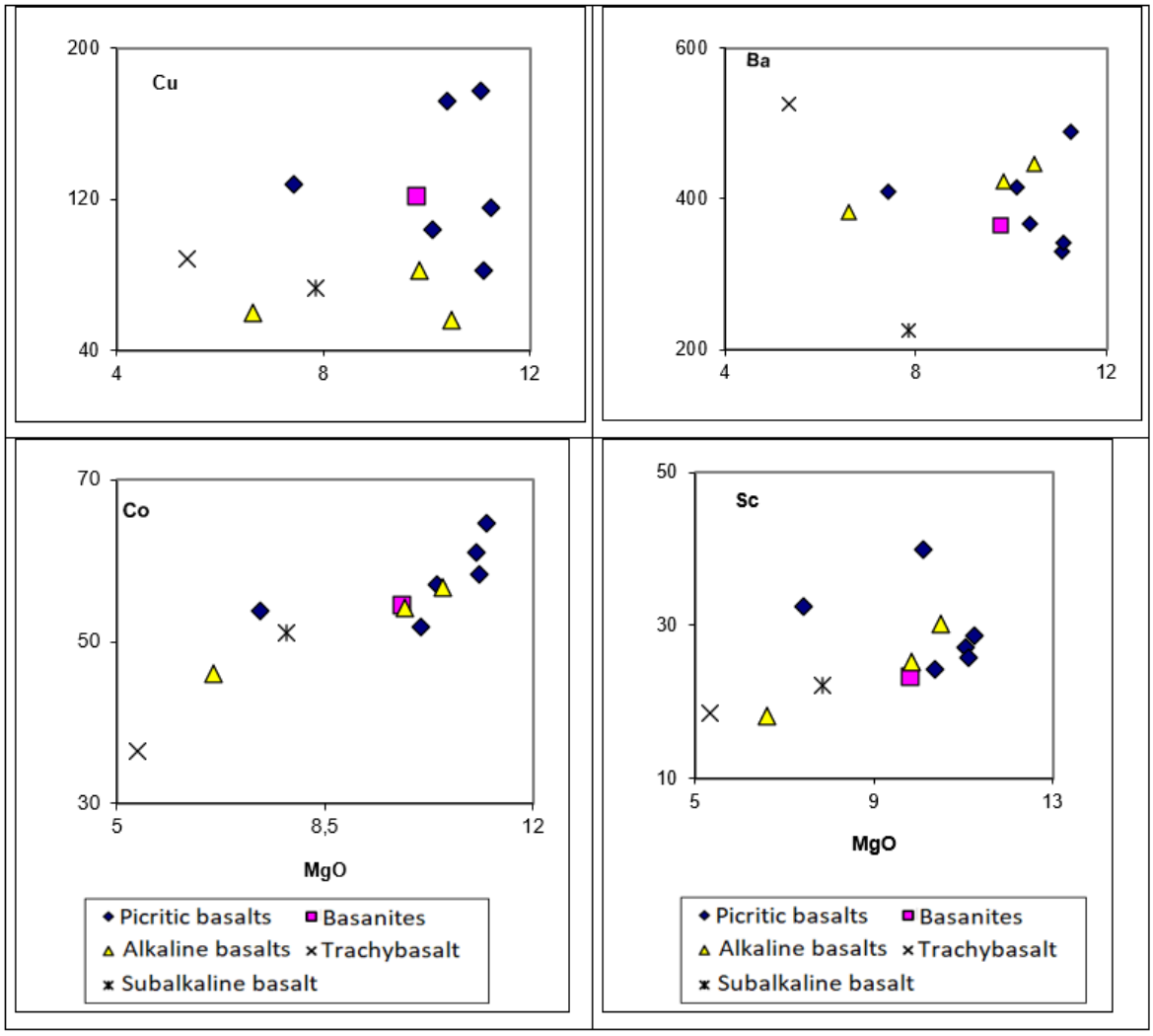
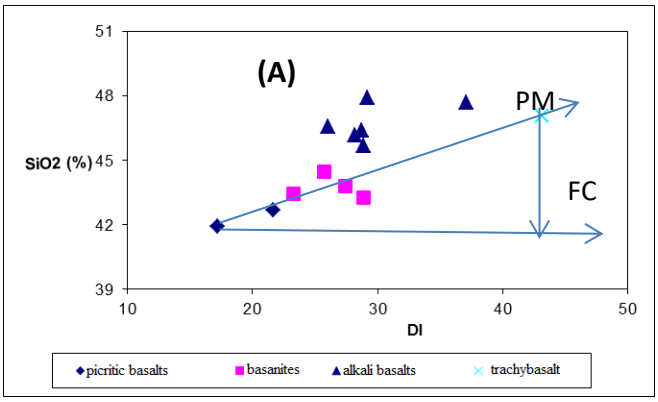


Figure 8. Variation diagrams of some trace elements (Co, Cu, Ba, Sc in ppm) as a function of MgO (%).



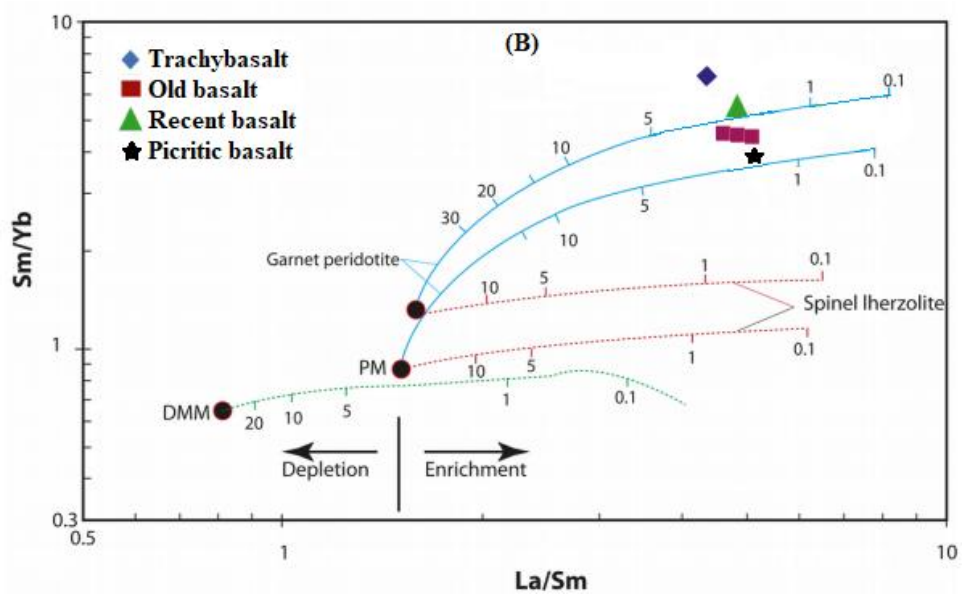


Figure 9. (**A**) Variation of SiO_2 as a function of DI. FC: Fractional Crystallization and empirical estimation of Partial Melting PM ≤ 4% (42% to 46% $Si0_2$, asymptote of fractional crystallization) ratio of alkaline basaltic magmas generated in intraplate settings [17] and (**B**) batch melting model, plot of the Kumba lavas in the Sm/Yb versus La/Sm diagram after Gurenko et al [50]. Values of DMM (Depleted MORB Mantle) are from Workman and Hart [51]. Values of PM are from Sun and McDonough [36]. The different curves represent the partial melting of garnet and spinel peridotites. The gradations represent the different melting rates. In the case of Kumba plain, PM (1.4 to 3.7%)